

Experimental and Semi-Analytical Investigation of Wave Interaction with Double Vertical Slotted Walls

H. Ahmed, A. Schlenkhoff, R. Roust, R. Abdelaziz

Abstract—Vertical slotted walls can be used as permeable breakwaters to provide economical and environmental protection from undesirable waves and currents inside the port. The permeable breakwaters are partially protection and have been suggested to overcome the environmental disadvantages of fully protection breakwaters. For regular waves a semi-analytical model is based on an eigenfunction expansion method and utilizes a boundary condition at the surface of each wall are developed to detect the energy dissipation through the slots. Extensive laboratory tests are carried out to validate the semi-analytic models. The structure of the physical model contains two walls and it consists of impermeable upper and lower part, where the draft is based a decimal multiple of the total depth. The middle part is permeable with a porosity of 50%. The second barrier is located at a distant of 0.5, 1, 1.5 and 2 times of the water depth from the first one. A comparison of the theoretical results with previous studies and experimental measurements of the present study show a good agreement and that, the semi-analytical model is able to adequately reproduce most the important features of the experiment.

Keywords—Permeable breakwater, double vertical slotted walls, semi-analytical model, transmission coefficient, reflection coefficient, energy dissipation coefficient.

I. INTRODUCTION

THE permeable breakwaters can be a sophisticated alternative to overcome the environmental disadvantages of fully protection breakwaters. The benefit of these structures is decreasing the transmission and energy of waves and consequently current inside a harbor and protect the coast lines. Large amount of energy is dissipated by the special geometry of barriers.

For many years, predictions of wave interactions with impermeable structures have been explored for the case of an impermeable breakwater on the basis of linear wave diffraction theory. Numerical solutions have been developed on the basis of the boundary element method [14] and the eigenfunction expansion method for linear wave [15], [1], [8], [9], [20], [2] [12] and nonlinear wave [3].

Hany Gomaa Ibrahim Ahmed, Dr. Eng., is with the Irrigation and Hydraulics dept., Al-Azhar Uni., Egypt. Postdoctoral researcher at Hydro Sciences (IGAW), Civil Eng. Dept., Bergische Uni. of Wuppertal, Germany (Mob. +201020970179; e-mail: hanygo3177@yahoo.com).

Andreas Schlenkhoff, Univ. Prof. Dr. Eng., is with the Waste Management & Hydro Sciences (IGAW), Civil Eng. Dept., Bergische Uni. of Wuppertal, Germany. (Tel: +49202-439-4234; Fax: +49202-439-4196; e-mail: schlenkh@uni-wuppertal.de).

RoosbehRousta, PhD candidate, is with the Waste Management & Hydro Sciences (IGAW), Civil Eng. Dept., Bergische University of Wuppertal, Germany, e-mail: roosbeh.rousta@uni-wuppertal.de

Ramadan Abdelaziz is with the Institute for Geology, Technische Uni. Bergakademie Freiberg, Freiberg, Germany.

Many researchers investigated the performance of partially immersed bodies and pile breakwaters numerically by using the Eigenfunction technique. Dalrymple et al. [5], Kakuno et al. [10], Isaacson et al. [9] and Park et al. [18] provided numerical solution for pile breakwaters. Abul-Azm [1] provided numerical solutions for thin semi-immersed breakwaters. Intensive efforts have been done to decrease unwanted wave transmission and increase the wave dissipation through the slots.

Since the wave interaction with a slotted vertical barrier is in center of interest, some researchers explored this structure to estimate the absorption of wave energy at free surface of the seabed (e.g. [19], [7], [4], [22]). Based on the physical shape of barrier the proportional of the porous barrier formulates a complex phase between velocity and pressure gradient. Moreover, Hagiwara [7]; Kriebel [13]; and Bennet et al. [4] compared gratefully the experimental data of transmission and reflection coefficient on the slotted barriers extending to the seabed. Partial submerged barriers extended to a distance from the sea surface are reported by Isaacson et al. [8].

Permeable barriers can not only reduce the wave reflection on upside the barrier but also wave transmission to an acceptable level. In order to achieve this purpose also two or more barriers can be employed, e.g. [21] and [15]. The wave interaction of a double screen breakwater was explored by [6]. Although, some studies compared theoretical and experimental results of double vertical slotted barriers for wave reflection and transmission, e.g. [11] and [7]. This sort of art need more efforts to discover new types that can dissipate a huge part of energy.

This paper deals with a semi-analytical model for regular waves to investigate the hydraulic performance of double vertical slotted wall. Extensive laboratory investigations are carried out to assess the semi-analytical model. A comparison of the theoretical results with previous studies of Isaacson et al. [9] and experimental measurements of the present study are conducted. It is also of interest to compare hydraulic performance of a single slotted wall [2] with a pair of them to improve the benefits of using the second wall.

II. THEORETICAL INVESTMENT

A linear wave propagates toward double vertical slotted wall breakwater. The first wall are located at distance of $(-\lambda)$ from the origin point, while the second wall located at a distance of (λ) as shown in Fig. 1. The velocity potential $\Phi(x, z, t)$ is a modified Laplace equation and “ Φ ” is assumed as a periodic motion in time T and it can be

$$\Phi(x, z, t) = \text{Re}(\frac{-igh_i}{2\omega}\phi(x, z)\frac{1}{\cosh kd}e^{-i\omega t}) \quad (1)$$

$$\frac{\partial \phi_1(x)}{\partial x} = \frac{\partial \phi_2(x)}{\partial x} = 0 \text{ at } x = -\lambda$$

or $-du \leq z \leq 0$ and $-d \leq z \leq -D$ (2)

$$\frac{\partial \phi_2(x)}{\partial x} = \frac{\partial \phi_3(x)}{\partial x} = 0 \text{ at } x = \lambda$$

$$-du \leq z \leq 0 \text{ and } -d \leq z \leq -D \quad (3)$$

$$\frac{\partial \phi_1(x)}{\partial x} = \frac{\partial \phi_2(x)}{\partial x} = iG^-(\phi_1(x) - \phi_2(x))$$

$$\text{at } x = -\lambda \text{ for } -D \leq z \leq -du \quad (4)$$

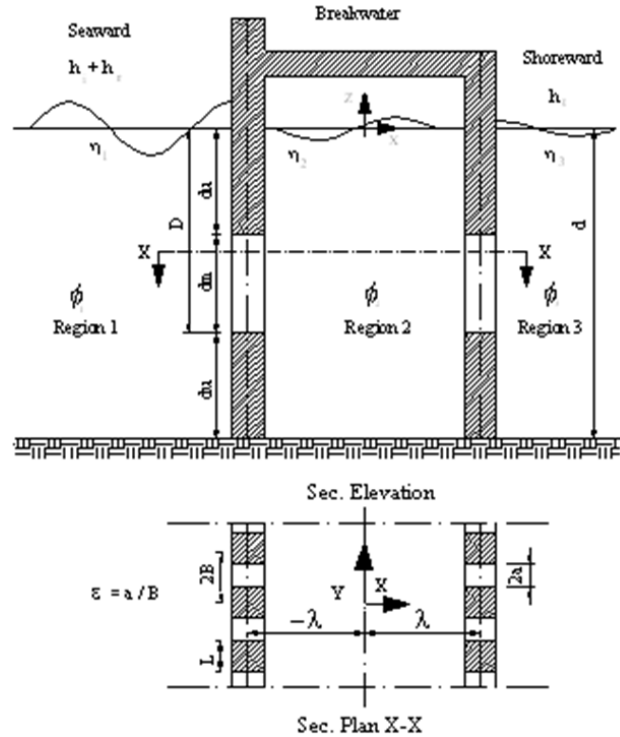
$$\frac{\partial \phi_2(x)}{\partial x} = \frac{\partial \phi_3(x)}{\partial x} = iG^-(\phi_2(x) - \phi_3(x))$$

$$\text{at } x = \lambda \text{ for } -D \leq z \leq -du \quad (5)$$

where $G = \frac{G}{b}$ is the proportional constant, G is called the permeability parameter and it is defined as $G = \frac{\varepsilon}{f - is}$ and $s = 1 + C_m \frac{1 - \varepsilon}{\varepsilon}$.

$$\begin{aligned} \phi_1(x) &= \phi_i + \sum_{m=0}^{\sigma} A_{1m} \cos[\mu_m(d+z)] \exp(\mu_m(x+\lambda)) \\ &\text{at } x \leq -\lambda \end{aligned} \quad (6)$$

$$\begin{aligned} \phi_2(x) = & \sum_{m=0}^{\infty} A_{2m} \cos[\mu_m(d+z)] \exp(-\mu_m(x+\lambda)) + \\ & \sum_{m=0}^{\infty} A_{3m} \cos[\mu_m(d+z)] \exp(\mu_m(x-\lambda)) \\ & \text{at } -\lambda \leq x \leq \lambda \end{aligned} \quad (7)$$



$$\phi_3(x) = \sum_{m=0}^{\infty} A_{4m} \cos[\mu_m(d+z)] \exp(-\mu_m(x-\lambda))$$

$$\text{at } -x \geq \lambda \quad (8)$$

$$\mu_m \sum_{m=0}^{\infty} A_{lm} \cos[\mu_m(d+z)] = \mu_o \cos[\mu_o(d+z)] \exp(\mu_o \lambda)$$

at $x \leq -\lambda$ for $-du \leq z \leq 0$ and $-d \leq z \leq -D$ (9)

$$\mu_m \sum_{m=0}^{\infty} A_{2m} \cos[\mu_m(d+z)] - \mu_m \sum_{m=0}^{\infty} A_{3m} \cos[\mu_m(d+z)] \exp(-2\mu_m \lambda) = 0$$

at $x \leq -\lambda$ for $-d \leq z \leq -D$ and $-du \leq z \leq 0$ (10)

$$\mu_m \sum_{n=0}^{\infty} A_{2m} \cos[\mu_m(d+z)] \exp(-2\mu_m \lambda) - \mu_m \sum_{n=0}^{\infty} A_{3m} \cos[\mu_m(d+z)] = 0$$

at $x \geq \lambda$ for $-du \leq z \leq 0$ and $-d \leq z \leq -D$ (11)

$$\mu_m \sum_{m=0}^{\infty} A_{4m} \cos[\mu_m(d+z)] = 0$$

at $x \leq \lambda$ for $-du \leq z \leq 0$ and $-d \leq z \leq -D$ (12)

Also:

$$(\mu_m - iG^-) \sum_{m=0}^{\infty} A_{1m} \cos[\mu_m(d+z)] + iG^- \sum_{m=0}^{\infty} A_{2m} \cos[\mu_m(d+z)] +$$

$$iG^- \sum_{m=0}^{\infty} A_{3m} \cos[\mu_m(d+z)] \exp(-2\lambda\mu_m) =$$

$$(iG^- + \mu_o) \exp(\mu_o\lambda) \cos[\mu_o(d+z)]$$

$$\text{at } x \leq -\lambda \text{ for } -D \leq z \leq -du \quad (13)$$

$$(iG^-) \sum_{m=0}^{\infty} A_{1m} \cos[\mu_m(d+z)] + (\mu_m - iG^-) \sum_{m=0}^{\infty} A_{2m} \cos[\mu_m(d+z)] -$$

$$(iG^- + \mu_m) \sum_{m=0}^{\infty} A_{3m} \cos[\mu_m(d+z)] \exp(-2\lambda\mu_m) =$$

$$- (iG^-) \exp(\mu_o\lambda) \cos[\mu_o(d+z)]$$

$$\text{at } x \leq -\lambda \text{ for } -D \leq z \leq -du \quad (14)$$

$$(\mu_m + iG^-) \sum_{m=0}^{\infty} A_{2m} \cos[\mu_m(d+z)] \exp(-2\lambda\mu_m) -$$

$$(\mu_m - iG^-) \sum_{m=0}^{\infty} A_{3m} \cos[\mu_m(d+z)] -$$

$$- iG^- \sum_{m=0}^{\infty} A_{4m} \cos[\mu_m(d+z)] = 0$$

$$\text{at } x \leq \lambda \text{ for } -D \leq z \leq -du \quad (15)$$

$$(iG^-) \sum_{m=0}^{\infty} A_{2m} \cos[\mu_m(d+z)] \exp(-2\lambda\mu_m) +$$

$$iG^- \sum_{m=0}^{\infty} A_{3m} \cos[\mu_m(d+z)] + (\mu_m - iG^-) \sum_{m=0}^{\infty} A_{4m} \cos[\mu_m(d+z)] = 0$$

$$\text{at } x \leq \lambda \text{ for } -D \leq z \leq -du \quad (16)$$

All of the above equations are integrated with respect to z over the appropriate domain of z . For the present article $z = -du$ to 0.0 , $z = -D$ to $-du$ and $z = -d$ to $-D$. Then, each resulting equation should be multiplied by $\cos[\mu_n(d+z)]$, and then added to obtain two sets of equation for A_{im} . Thus the matrix equation for A_{1m} , A_{2m} , A_{3m} and A_{4m} will be:

$$\begin{bmatrix} \sum_{m=0}^{\infty} C_{11}^{(mn)} & \sum_{m=0}^{\infty} C_{12}^{(mn)} & \sum_{m=0}^{\infty} C_{13}^{(mn)} & \sum_{m=0}^{\infty} C_{14}^{(mn)} \\ \sum_{m=0}^{\infty} C_{21}^{(mn)} & \sum_{m=0}^{\infty} C_{22}^{(mn)} & \sum_{m=0}^{\infty} C_{23}^{(mn)} & \sum_{m=0}^{\infty} C_{24}^{(mn)} \\ \sum_{m=0}^{\infty} C_{31}^{(mn)} & \sum_{m=0}^{\infty} C_{32}^{(mn)} & \sum_{m=0}^{\infty} C_{33}^{(mn)} & \sum_{m=0}^{\infty} C_{34}^{(mn)} \\ \sum_{m=0}^{\infty} C_{41}^{(mn)} & \sum_{m=0}^{\infty} C_{42}^{(mn)} & \sum_{m=0}^{\infty} C_{43}^{(mn)} & \sum_{m=0}^{\infty} C_{44}^{(mn)} \end{bmatrix} \begin{bmatrix} A_{1m} \\ A_{2m} \\ A_{3m} \\ A_{4m} \end{bmatrix} = \begin{bmatrix} b_{1n} \\ b_{2n} \\ b_{3n} \\ b_{4n} \end{bmatrix}$$

For $n=1, 2, 3, \dots, \infty$ (17)

where:

$$C_{11} = \mu_m [\delta_{mn}^-(du, 0) + \delta_{mn}^-(d, -D)] + (\mu_m - iG^-) \delta_{mn}^-(D, -du) \quad (18)$$

$$C_{12} = (iG^-) \delta_{mn}^-(D, -du) \quad (19)$$

$$C_{13} = (iG^-) \exp(-2\lambda\mu_m) \delta_{mn}^-(D, -du) \quad (20)$$

$$C_{14}; C_{24}; C_{31}; C_{41} = 0 \quad (21)$$

$$C_{21} = (iG^-) \delta_{mn}^-(D, -du) \quad (22)$$

$$C_{22} = \mu_m [\delta_{mn}^-(du, 0) + \delta_{mn}^-(d, -D)] + (\mu_m - iG^-) \delta_{mn}^-(D, -du) \quad (23)$$

$$C_{23} = \mu_m \exp(-2\lambda\mu_m) [\delta_{mn}^-(du, 0) + \delta_{mn}^-(d, -D)] +$$

$$(iG^- + \mu_m) \exp(-2\lambda\mu_m) \delta_{mn}^-(D, -du) \quad (24)$$

$$C_{32} = \mu_m \exp(-2\lambda\mu_m) [\delta_{mn}^-(du, 0) + \delta_{mn}^-(d, -D)] +$$

$$(iG^- + \mu_m) \exp(-2\lambda\mu_m) \delta_{mn}^-(D, -du) \quad (25)$$

$$C_{33} = -\mu_m [\delta_{mn}^-(du, 0) + \delta_{mn}^-(d, -D)] + (iG^- - \mu_m) \delta_{mn}^-(D, -du) \quad (26)$$

$$C_{34} = (-iG^-) \delta_{mn}^-(D, -du) \quad (27)$$

$$C_{42} = (iG^-) \exp(-2\lambda\mu_m) \delta_{mn}^-(D, -du) \quad (28)$$

$$C_{43} = (iG^-) \delta_{mn}^-(D, -du) \quad (29)$$

$$C_{44} = \mu_m [\delta_{mn}^-(du, 0) + \delta_{mn}^-(d, -D)] + (\mu_m - iG^-) \delta_{mn}^-(D, -du) \quad (30)$$

$$b_{1n} = \mu_o \exp(\lambda\mu_o) \delta_{on}^-(du, 0) + \delta_{on}^-(D, -du) +$$

$$(iG^- + \mu_o) \exp(\lambda\mu_o) \delta_{on}^-(d, -D) \quad (31)$$

$$b_{2n} = (-iG^-) \exp(\lambda\mu_o) \delta_{on}^-(d, -D) \quad (32)$$

$$b_{3n} = b_{4n} = 0 \quad (33)$$

$$\delta_{mn}^-(p, q) = \int_p^q \cos[\mu_m(d+z)] \cos[\mu_n(d+z)] dz \quad (34)$$

$$= \begin{cases} \frac{1}{2} \left\{ \frac{\sin[(\mu_m + \mu_n)(d+z)]}{\mu_m + \mu_n} + \frac{\sin[(\mu_m - \mu_n)(d+z)]}{\mu_m - \mu_n} \right\}_p^q & \text{for } m \neq n \\ \frac{1}{4\mu_m} [2\mu_m(d+z) + \sin[2\mu_m(d+z)]]_p^q & \text{for } m = n \end{cases} \quad (35)$$

The matrix (17) is becomes a complex matrix equation of rank $4N$, which can be calculated for the first N unknown values of each set coefficient A_{1m} , A_{2m} , A_{3m} and A_{4m} . The real reflection (CR) and transmission coefficients (CT), are assumed in terms of A_{1m} and A_{4m} by:

$$CR = |A_{10}| \quad (36)$$

$$CT = |A_{40}| \quad (37)$$

The energy losses coefficient (CE) is given by:

$$CE = 1 - (CR^2 + CT^2) \quad (38)$$

III. DESCRIPTION OF EXPERIMENTS

For investigation the wave interaction with breakwaters many experiments have been conducted in a wave flume at the hydraulic engineering section of the Bergische University of Wuppertal-Germany (Fig. 1). The glassed wall flume is 24m long, 0.30m wide, 0.5m deep but water depth of $d = 0.3$ m. The proposed permeable breakwater model is a pair of vertical slotted walls as shown in Fig. 2.



Fig. 2 Photograph of wave flume

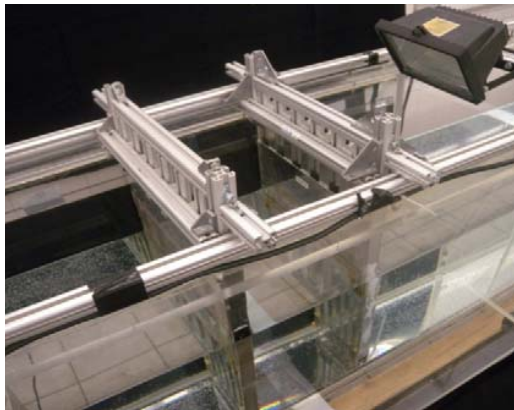


Fig. 3 View of double vertical slotted wall model

Every wall constructed of vertical panels with width of 2.5 cm, and thickness of 2.5 cm. In fact, the porosity of the barriers is 50% in the middle part. Also, the draft of the permeable area varies as a proportion of the water depth ($dm = 0.2d, 0.4d, 0.6d$ and $0.8d$). The upper and lower parts are impermeable with different draft changes according to dm . The regular waves with different frequencies of 0.5, 0.75, 1.0, 1.25, 1.5, 1.75 and 2.0 Hz, and also corresponding wave height of 1.0, 1.0, 2.0, 2.0, 3.0, 4.0 and 4.0 cm are examined. Moreover, the chamber width varies as proportion of the water

depth ($2\lambda = 0.5, 1.0, 1.5$ and $2.0d$). First, three sensors were kept in front of the model at a distance more than the longest wave length considered in the testing program. The spacing between the first three probes are adjusted for each of the wave period so as to calculate the reflection coefficient by the three-probe method of Mansard and Funke [16]. The wave transmission is recorded by a sensor kept at the rear side of the model at a distance of about the longest wavelength considered for testing purpose. All readings are taken before the impact of the absorber of the wave paddle and the flume end by examining the plotted wave's records and using the approximate arrival time of the first reflected wave.

IV. RESULTS AND DISCUSSION

A. Validation

The validation of semi-analytical model has been done by a comparison with the experimental and theoretical results of Isaacson et al. [8] as show in Fig. 4. This comparison is carried out to investigate the hydrodynamic characteristics of two identical barrier through hydrodynamic characteristics CR , CT and CE coefficients as a function of $k.du$. The configuration of this comparison are; $hi/L = 0.07$, $f = 2$, $cm = 0.00$, $b = 1.3$ cm, $d = 0.45$ cm and barrier spacing $\lambda = 1.1 du$.

The agreement between the present study and the results of Isaacson et al. [8] is found to be excellent despite small differences of CT in long waves. The present study show better convergence to experimental results of Isaacson et al. [8] more than his theoretical.

B. Influence of the Permeable Depth

The influence of the permeable part " dm " on the hydrodynamic characteristics of identical double vertical slotted walls is plotted in Figs. 5-10, which indicate the comparison of the measured and predicted transmission, reflection, and energy dissipation coefficients as a function of kd as shown in Figs. 5-8 and as a function of dm/d as shown in Figs. 9 and 10. The wave steepness is $hi/L = 0.025$, the upper and lower parts are impermeable, various permeability draft examined as a water depth $dm = 0.8, 0.6, 0.4$ and $0.2 d$. Obviously, The draft of the upper and lower parts changed according to dm . However, the values of the friction and the addition mass coefficient can be taken as mean value of $f = 2$ and $cm = 0$ within this configuration on the basis of a best fit between the measured and predicted values of the transmission, reflection and energy dissipation coefficients. The chamber width varies as a proportion of the water depth = 0.5, 1, 1.5 and $2d$, as shown in Figs. 5-8.

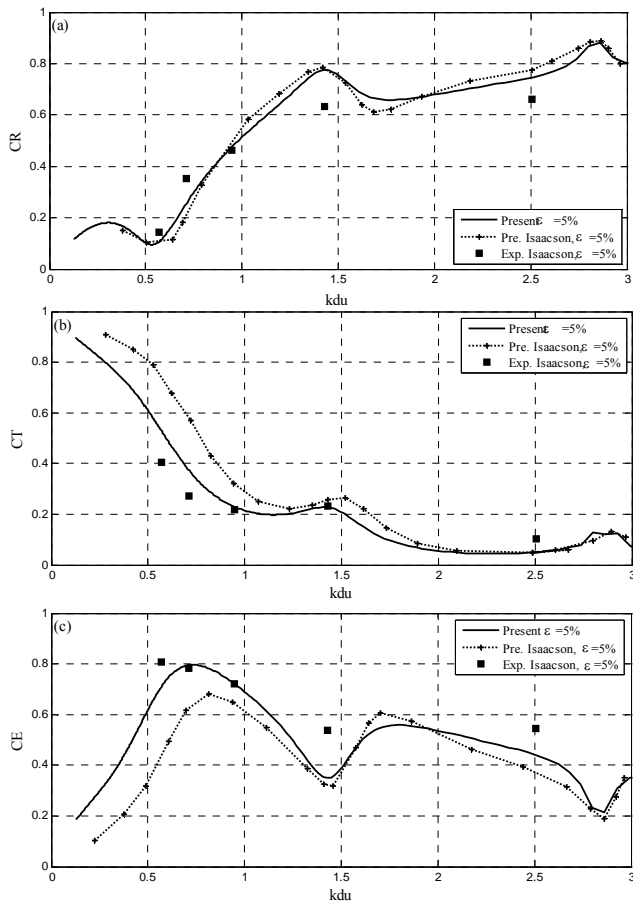


Fig. 4 Comparison of the present model with results of Isaacson et al. [8] (a) CR , (b) CT and (c) CE

In general, the reflection coefficient, CR increases with increasing kd at fixed dm and also increases with decreasing dm at fixed kd . However, the trend of the transmission coefficient, CT is opposite and is less for the model when the $dm = d$ (i.e. a pile case) and is maximum for $dm = 0.00$ (i.e. the reflection coefficient = 100% for the wall), while the transmission coefficient for this case is $CT = 0$. It is obvious that the reflection and transmission coefficients are approximately counter parameters with value between 0 and 1. It means, when the former's value increases and approaches 1, the latter's value decreases and comes close to 0 and vice versa. For clarifying the effect of the portion of the permeability for example at $kd = 1$, the reflection changes from 25% to 58%, relatively transmission coefficient varies from 75% to almost 30%. The energy dissipation, CE gradually increases with increasing kd for the lower kd and because of second barrier the dissipation rate rises to more than 80%.

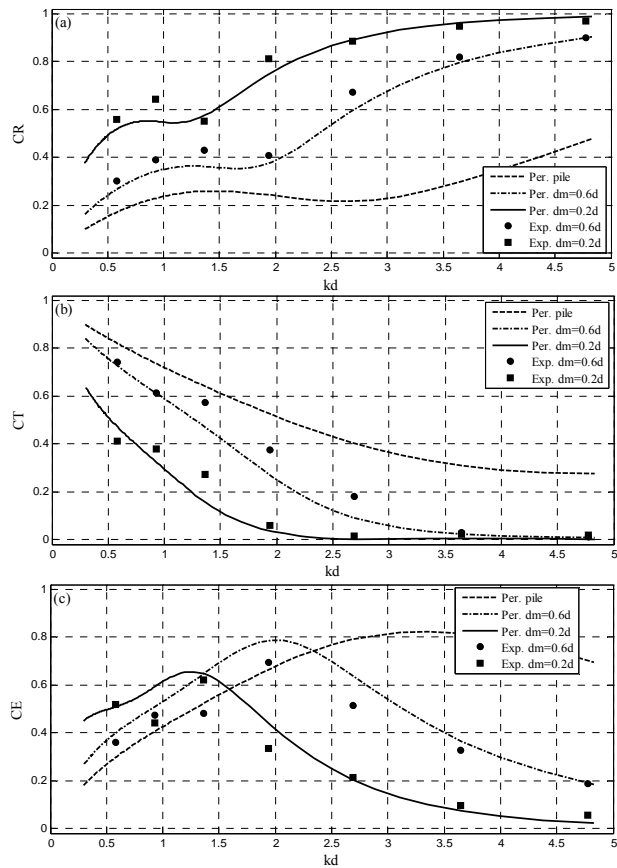


Fig. 5 Comparison of prediction and experimental results as function kd , at $\lambda/d = 0.25$. (a) CR , (b) CT and (c) CE

The differences between the measured and predicted results are most notable in the energy loss coefficients. Note that the energy loss coefficient is calculated directly from the measured transmission and reflection coefficients so that the scatter in the measured values is due in part to experimental errors in measuring the transmitted and reflected waves. Interestingly, the peaks in CR , CT , and CE charts are observed and the number of peaks rises with increasing the chamber width. For larger relative spacing, peaks in the transmission and reflection coefficients occur when the relative draft $kd = n\pi / (2\lambda/d)$, corresponding to resonant excitation of partial standing waves between the barriers. This result agrees with the result of double slotted barriers [8].

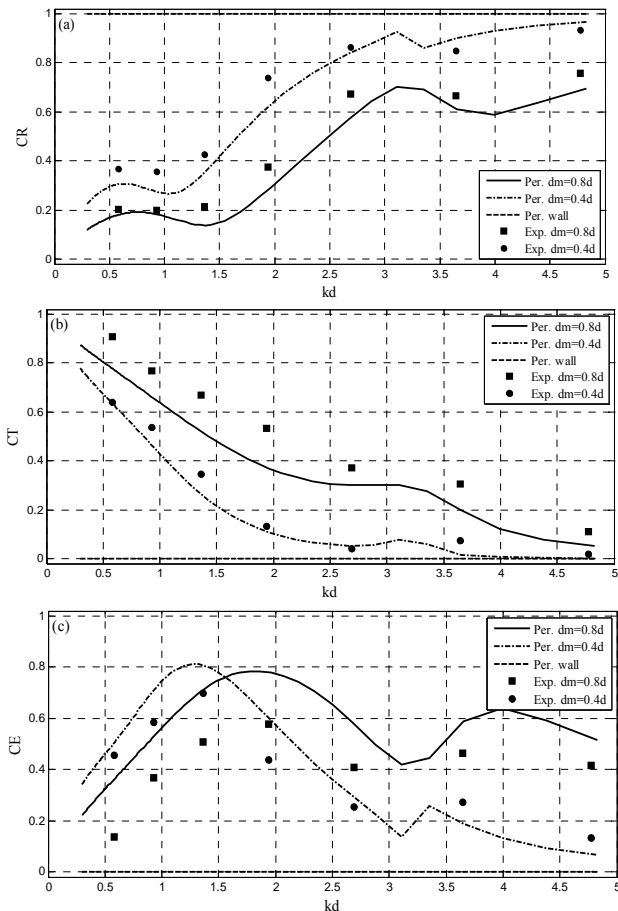


Fig. 6 Comparison of prediction and experimental results as function kd , at $\lambda/d = 0.5$. (a) CR , (b) CT and (c) CE

The effect of the permeability part is also presented as a function of the relative middle permeable part dm/d for different chamber width as a proportion of the water depth as shown in Figs. 8, 9. The middle part is permeable with porosity $\varepsilon = 50\%$ and various draft $dm = 0.2d$, for different $kd = 4.772$ and 0.577 . In general, choice of the opening area is particularly important. The reflection coefficient, CR decreases with increasing dm/d while the transmission coefficient, CT follows the opposite trend. Therefore, the efficiency of this type surpasses the efficiency of double rows of pile breakwater, which has the same porosity. The target protection can be achieved through the best choice for the permeability area.

Overall, the agreement of the results is satisfactory when the chamber width is a proportion of the water depth, although there is some scatter between the experimental and predicted results. Therefore, the numerical model is able to adequately reproduce the most important features of the experimental results, including the energy dissipation through the double vertical slotted barrier.

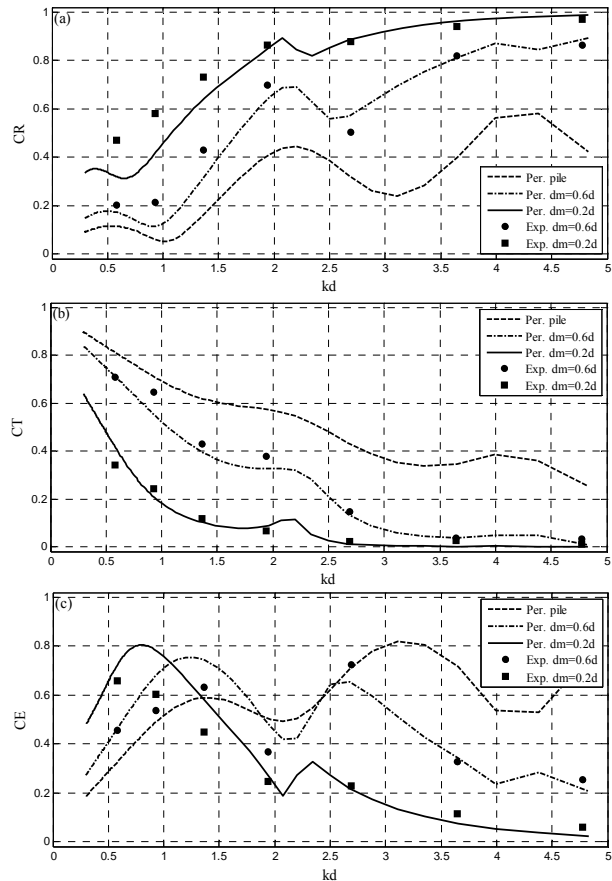


Fig. 7 Comparison of prediction and experimental results as function kd , at $\lambda/d = 0$. (a) CR , (b) CT and (c) CE

C. Influence of Addition the Second Wall

It is also crucial to compare the influence of double vertical slotted walls with the single wall. Figs. 11, 12 show a comparison of the transmission, reflection and energy dissipation coefficients of single and double vertical slotted wall as functions of kd , for various $\lambda/d = 0.25, 0.5, 0.75$ and $d, f = 2.0, cm = 0.00, \varepsilon = 50\%$ and $dm = 0.2d, 0.4d, 0.6d$ and $0.8d$ as shown in Figs. 10 and 11 respectively. As expected, the addition of the second barrier has no distinct influence on the reflection coefficient but has special and distinct influence on the transmission and energy dissipation coefficient. It is noted that there is a noticeable decrease in the transmission coefficient up to 30 % and a noticeable increase in the energy dissipation coefficient up to 40 %, because the second wall dissipate an additional part from the energy of the wave. Furthermore, it gives the least reflection coefficient, which leads to decrease the force on the wall as well as to decrease the transmission of waves inside the harbor. Finally, the efficiency of this type surpasses the efficiency of a single vertical wall, which has the same parameter in all cases.

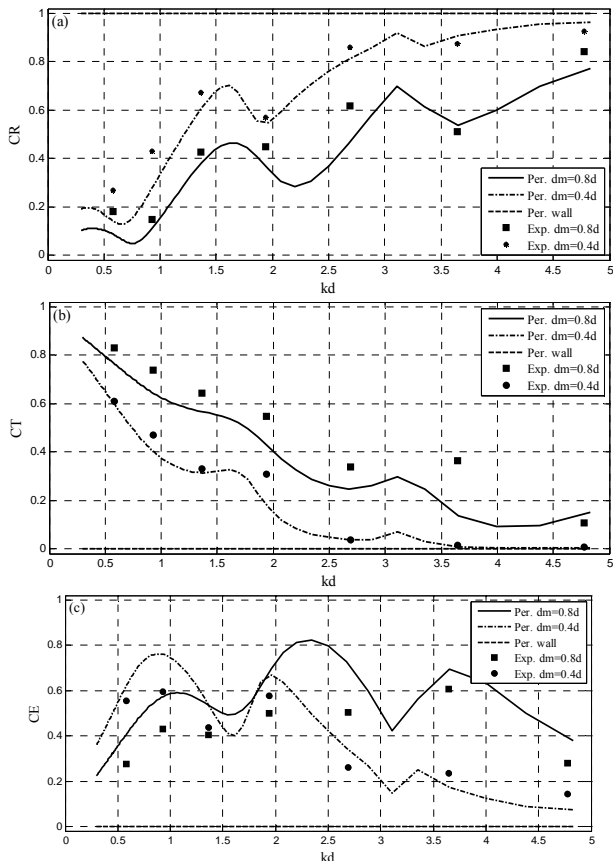


Fig. 8 Comparison of prediction and experimental results as function kd , at $\lambda/d = 0$. (a) CR , (b) CT and (c) CE

V.CONCLUSION

This study describes the hydrodynamic characteristics of linear wave interaction with double vertical slotted walls. For regular wave, an Eigenfunction expansion method has been developed to predict various hydrodynamic characteristics (CR , CT and CE). The semi-analytical model is validated by comparison with results of Isaacson et al. [8] and experimental results.

A comparison between the hydraulic performance of a single and double vertical slotted walls breakwaters has been conducted.

Comparisons of corresponding semi-analytical results of CR , CT and CE with experimental results showed that the agreement is generally satisfactory and indicates that the numerical model is able to adequately reproduce most of the important features of the experimental results.

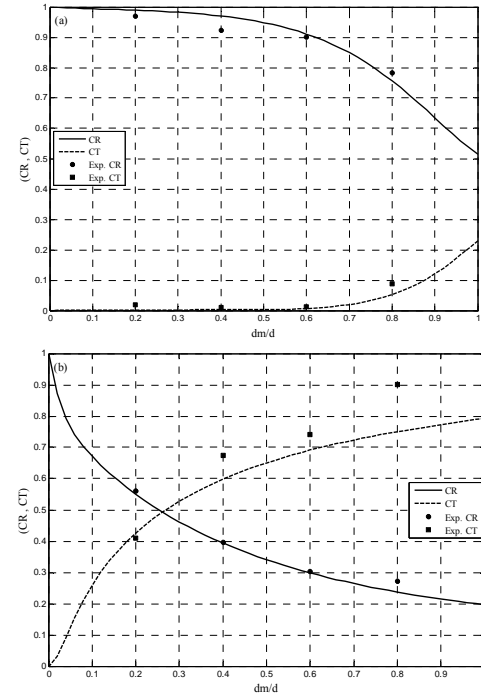


Fig. 9 Comparison between measured and predicted reflection and transmission coefficients for $\lambda/d = 0.25$. (a) $T = 0.5$ sec, (b) $T = 2$ sec

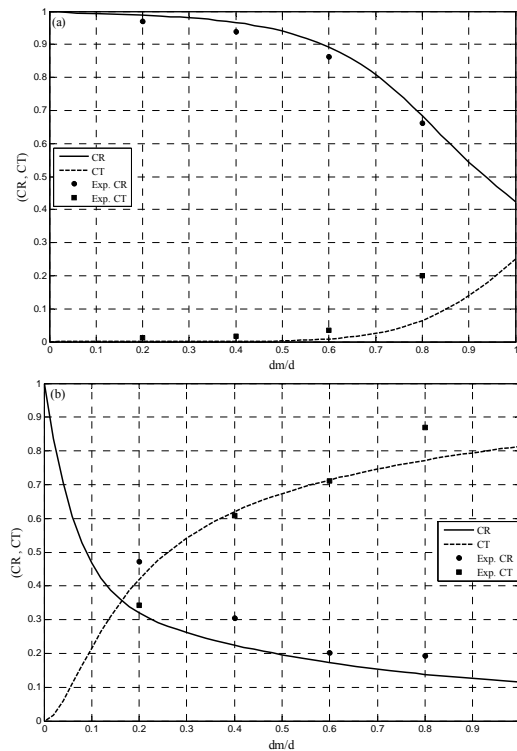


Fig. 10 Comparison between measured and predicted reflection and transmission coefficients for $\lambda/d = 0.75$. (a) $T = 0.5$ sec, (b) $T = 2$ sec

The reflection coefficient, CR increases with increasing kd at fixed dm and increases with decreasing dm at fixed kd . The

transmission coefficient, CT follows the opposite trend. The energy dissipation, CE slowly increases with increasing kd for the lower kd and reaches more than 80 % because the second barrier causes additional vortex, which dissipate more wave energy. The target protection can be achieved through the best choice for the permeability area.

The efficiency of this type surpasses the efficiency of double rows of pile breakwater, which has the same porosity. The addition of the second barrier has no distinct influence on CR but has distinct influence on CT and CE . A noticeable decrease in CT up to 30% and a noticeable increase in the energy dissipation coefficient up to 40%, were remarked because the second wall dissipate additional part from the energy of wave.

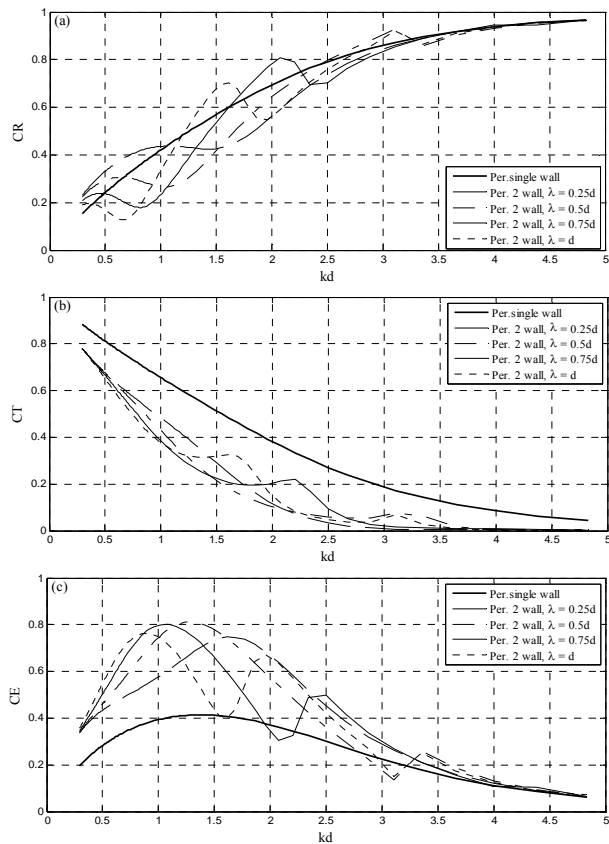


Fig. 11 Comparison between prediction results of single model [2] and double vertical slotted wall as function of (kd) for various λ/d (a) CR , (b) CT and (c) CE

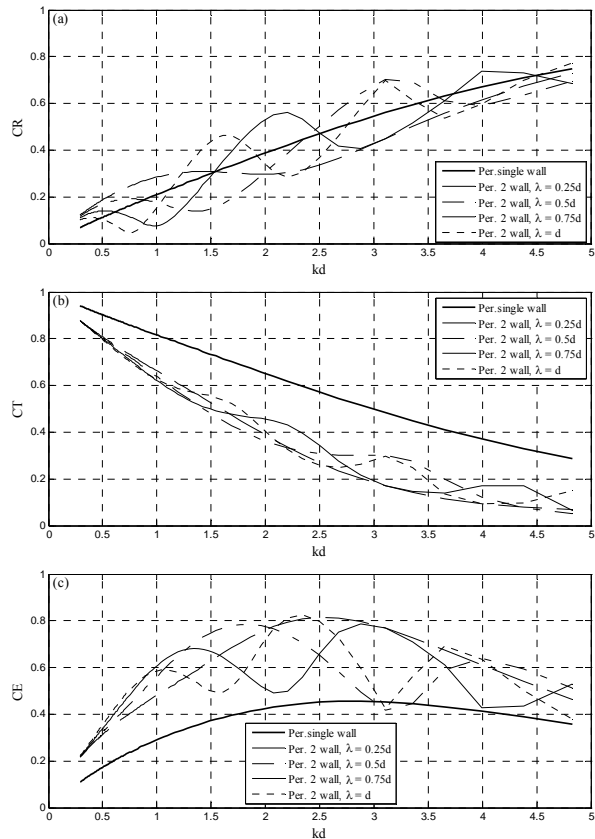


Fig. 12 Comparison between prediction results of single model [2] and double vertical slotted wall as function of (kd) for various λ/d . (a) CR , (b) CT and (c) CE

REFERENCES

- [1] R. G. Abul-Azm, "Wave diffraction through submerged breakwaters," *Waterway, Port, Coastal and Ocean. J.*, vol. 119, no. 6, pp. 587–605, 1993.
- [2] H. G. Ahmed, A. Schlenkhoff, and D. Bung, "Hydrodynamic characteristics of vertical slotted wall breakwaters," *34th IAHR World Congress, Brisbane – Australia*, 2011.
- [3] H. G. Ahmed, A. Schlenkhoff, M. Oertel, "Stokes second-order wave interaction with vertical slotted wall breakwater," *Coastal structures Conf. Yokohama, Japan*, 2011.
- [4] G.S. Bennett, P. McIver, and J. V. Smallman, "A mathematical model of a slotted wave screen breakwater," *Coastal Eng. J.*, vol. 18, pp. 231–249, 1992.
- [5] R. A. Dalrymple, M.A. Losada and P.A. Martin, "Reflection and transmission from porous structures under oblique wave attack," *Fluid Mech. J.*, vol. 224, pp. 625–644, 1991.
- [6] J. Gardner, I. Townend and C. Fleming, "The design of a slotted vertical screen breakwater," *Proc. 20th Coastal Eng. Conf., ASCE, Taipei*, pp. 1881–1893, 1986.
- [7] K. Hagiwara, "Analysis of upright structure for wave dissipation using integral equation," *Proc., 19th Int. Conf. on Coastal Engineering (ICCE), ASCE, Reston, Va.*, pp. 2810–2826, 1984.
- [8] M. Isaacson, J. Baldwin, S. Premasiro and G. Yang, "Wave interaction with double slotted barriers," *Applied Ocean Research. J.*, vol. 21, no. 2, pp. 81–91, 1999.
- [9] M. Isaacson, S. Premasiro and G. Yang, "Wave interaction with vertical slotted barrier," *Waterway, Port, Coastal and Ocean. J.*, vol. 124, no. 3, pp. 118–126, 1998.
- [10] S. Kakuno, and P.L.F. Liu, "Scattering of water waves by vertical cylinders," *Waterway, Port, Coastal and Ocean. J., ASCE*, vol. 119, 1993.

- [11] H. Kondo, "Analysis of breakwaters having two porous walls," *Proc. Coastal Structures '79*, ASCE, Arlington, pp. 939–952, 1979.
- [12] A. S. Koraim, E. M. Heikal, OS. Rageh, "Hydrodynamic characteristics of double permeable breakwater under regular waves," *Coastal Engineering J.*, vol. 24, pp. 503–527, 2011.
- [13] D. L. Kriebel, "Vertical wave barriers: Wave transmission and wave forces," *23rd Int. Conf. on Coastal Eng.*, ASCE, vol. 2, pp. 1313–1326, 1992.
- [14] PL-F. Liu, and M. Abbaspour, "Wave scattering by a rigid thin barrier," *Waterway, Port, Coastal and Ocean Eng. J. Div. ASCE*, vol. 108, no. 4, pp. 479–491, 1982.
- [15] I. J. Losada, M. A. Losada, and A. Baquerizo, "An analytical method to evaluate the efficiency of porous screens as wave dampers," *Applied Ocean Research*, no. 15, pp. 207–215, 1993.
- [16] E. P. D. Mansard, and E. R. Funke, "The measurement of incident and reflected spectra using a least squares method," *In Proc. 17th Coastal Eng. Conf.*, Sydney, Australia, pp. 159–174, 1980.
- [17] T. Nakamura, T. Kohno, K. Makimoto, H. Kamikawa, "Enhancement of wave energy dissipation by a double curtain-walled breakwater with different drafts," *Proc. of Coastal Structures 99*, Rotterdam, pp. 533–540, 1999.
- [18] W. S. Park, B. Kim, K. Suh, and K. Lee, "Irregular wave scattering by cylinder breakwaters," *Korea-China Conf. on Port and Coastal Eng.*, Seoul, Korea, 2000.
- [19] C. K. Sollitt, and R. H. Cross, "Wave transmission through permeable breakwaters," *Proc. of the 13th Coastal Eng. Conf.*, ASCE, Vancouver, pp. 1827–1846, 1972.
- [20] K. D. Suh, S. Shin and D. T. Cox, "Hydrodynamic characteristics of pile-Supported vertical wall breakwaters," *Waterways, Port, Coastal and Ocean Engineering J.*, vol. 132, no. 2, pp. 83–96, 2006.
- [21] S. W. Twu, and D. T. Lin, "Wave reflection by a number of thin porous plates fixed in a semi-infinitely long flume," *Proc. 22nd Coastal Eng. Conf.*, ASCE, Delft, pp. 1046–1059, 1990.
- [22] X. Yu, "Diffraction of water waves by porous breakwater," *Waterway, Port, Coastal and Ocean Engineering J.*, vol. 121, no. 6, pp. 275–282, 1995.